# Influence of Counter-ions on Antifogging Coatings

by

Shashank Sundareshan

SUBMITTED TO THE DEPARTMENT OF MATERIALS SCIENCE AND ENGINEERING IN PARTIAL FULFILLMENT OF THE REQUIREMENTS FOR THE DEGREE OF

BACHELOR OF SCIENCE
AT THE
MASSACHUSETTS INSTITUTE OF TECHNOLOGY

MAY 2008
[June 2008]





Signature of Author _____
Department of Materials Science and Engineering
May 9, 2008

Certified by _____
Michael F. Rubner
Professor of Materials Science and Engineering
Thesis Supervisor

Accepted by _____
Caroline A. Ross
Professor of Materials Science and Engineering
Chair, Departmental Undergraduate Committee

# Influence of Counter-ions on Antifogging Coatings

by

Shashank Sundareshan

Submitted to the Department of Materials Science and Engineering on May 9, 2008 in Partial Fulfillment of the Requirements for the degree of Bachelor of Science in Materials Science and Engineering.

**Abstract**

The influence of different counter-ions on the superhydrophilic and antifogging behavior of polyelectrolyte multilayers was examined. Multilayers assembled with a polymer anion and amine-modified silica nanoparticles were treated with salt solutions of monovalent and divalent cations. Refraction index of the films dropped significantly when treated with monovalent cations, and increased when treated with divalent cations. It has been found that the refraction index decrease in films treated with monovalent salts may be correlated with porosity increase in treated films, and this porosity increase in turn linked with an increase in hydrophilicity. Polyelectrolyte films have yet to show long-lasting antifogging properties on the commercially valuable polycarbonate, but monovalent cations may have improved the longevity of antifogging properties of the multilayer on polycarbonate, and warrant further study.

# TABLE OF CONTENTS

ABSTRACT ..... 2
TABLE OF CONTENTS ..... 3
LIST OF FIGURES AND TABLES ..... 4
ACKNOWLEDGEMENTS ..... 5
Chapter 1 Introduction ..... 6
1.1 Introductory Remarks ..... 6
1.2 Project Goals ..... 10
1.2.1 Thesis Objectives ..... 10
1.2.2 Thesis Motivation ..... 10
1.2.3 Current Research Advancements ..... 11
Chapter 2 Design Parameters ..... 12
2.1 Introduction to Design Idea ..... 12
2.2 Exploratory Experimentation ..... 12
2.2.1 Thickness Consideration and Calibration ..... 12
2.2.2 Free Carboxylic acid Group Content ..... 12
2.2.3 Film Stability Under pH Stress ..... 13
2.3 Exploratory Experimental Methods ..... 14
2.3.1 Polyelectrolyte Films on Glass Slides ..... 14
2.3.2 Film Stability Under pH Stress ..... 14
2.3.3 Free Carboxylic acid Group Content ..... 15
2.4 Exploratory Experimental Results ..... 15
2.5 Experimental Setup Conclusions ..... 19
Chapter 3 Counter-ion Influence on Antifogging PEMs ..... 19
3.1 Polyelectrolyte Films on Polycarbonate Slides ..... 19
3.2 Counter-ion Substitution ..... 20
3.3 Film Characterization ..... 20
3.3.1 Anti-Fog Test ..... 20
3.3.2 Contact Angle Measurement ..... 21
3.3.3 Durability Test ..... 21
3.3.4 Humidity Chamber Aging ..... 21
3.3.5 Ellipsometry Measurements ..... 21
3.4 Results ..... 22
3.5 Discussion ..... 28
Chapter 4 Summary and Future Work ..... 30
4.1 Thesis Summary ..... 30
4.2 Future Directions ..... 30
4.3 Bibliography ..... 31
Appendix A ..... 32

# LIST OF FIGURES AND TABLES

**Figure 1.** LbL growth process for a negatively charged substrate ..... 6
**Figure 2.** Polyectrolyte charge dependence on pH ..... 8
**Figure 3.** APSiO2/PAA film on negatively charged substrate ..... 8
**Figure 4.** Introduction of cations to $APSiO_2$/PAA film (include x-linking) ..... 11
**Figure 5.** Methylene blue molecular structure ..... 13
**Figure 6.** Calibration curves for films grown at a) pH 3.0, b) pH 2.5, and c) pH 2.0 ..... 16-17
**Table 1.** Results of pH dips for different growth systems ..... 17-18
**Figure 7.** Degradation of pH treated films ..... 18
**Table 2.** Methylene blue stained absorbance results of post-assembly treated films ..... 18-19
**Figure 8.** Dynamic contact angles of counter-ion dipped films ..... 23-24
**Figure 9.** Final contact angles of counter-ion dipped films ..... 25
**Table 3.** Development of anti-fogging properties over humidity aging time ..... 26
**Figure 10.** Anti-fog test of unaltered, Na-modified, and Li-modified films ..... 26
**Table 4.** Mechanical Durability of counter-ion films under rubbing test ..... 27
**Table 5.** Film thickness and refractive index ..... 28
**Table 6.** Film thickness and refractive index without roughness layer ..... 28
**Figure 11.** Anti-fog tests on unaltered films before and during humidity aging ..... 32
**Figure 12.** Anti-fog tests on $Na^+$-modified films before and during humidity aging ..... 33
**Figure 13.** Anti-fog tests on $Li^+$-modified films before and during humidity aging ..... 34
**Figure 14.** Anti-fog tests on $K^+$-modified films before and during humidity aging ..... 35
**Figure 15.** Anti-fog tests on $Mg^{2+}$-modified films before and during humidity aging ..... 36
**Figure 16.** Anti-fog tests on $Ca^{2+}$-modified films before and during humidity aging ..... 37
**Figure 17.** Anti-fog tests on $Ba^{2+}$-modified films before and during humidity aging ..... 38

# ACKNOWLEDGEMENTS

I would like to thank my graduate student advisor, Zekeriyya Gemici, for all of his help in teaching me a variety of experimental techniques and data analysis and in guiding me to a better understanding of the project. Additionally, I would like to thank Jenny Lichter for training me in the methylene blue staining technique and analysis, as well as Tim McClure for training me to use a profilometer and spectrophotometer. This help proved invaluable in deciding which experimental setup to use. I would also like to thank Dr. Koushik Mukherjee and Hiroomi Shimomura for providing me materials with which to complete my polymer films. I especially want to thank Professor Michael F. Rubner for allowing me the opportunity to participate in such an exciting field and on such a meaningful and directly applicable topic. Lastly, I would like to thank the Department of Materials Science and Engineering, the Center for Materials Science and Engineering, and the Institute for Soldier Nanotechnology for allowing me access to state-of-the art characterization tools and facilities.

# Chapter 1: Introduction

## 1.1 Introductory remarks

Polyelectrolyte multilayers (PEMs) are films grown by layering alternately charged polyelectrolytes, or polymers with charged groups. Alternately, PEMs can be grown with a combination of polyelectrolytes and charged nanoparticles. Because of the great deal of engineering control available in the surface modification of these multilayer films, they have been heavily researched for a variety of novel uses including creating antibacterial, antifogging, and antireflective coatings, as well as uses in fuel cells. Properties such as thickness, composition, and porosity, can greatly alter the characteristics of the film. PEMs are typically grown using the Layer-by-Layer (LbL) method, shown in Figure 1.

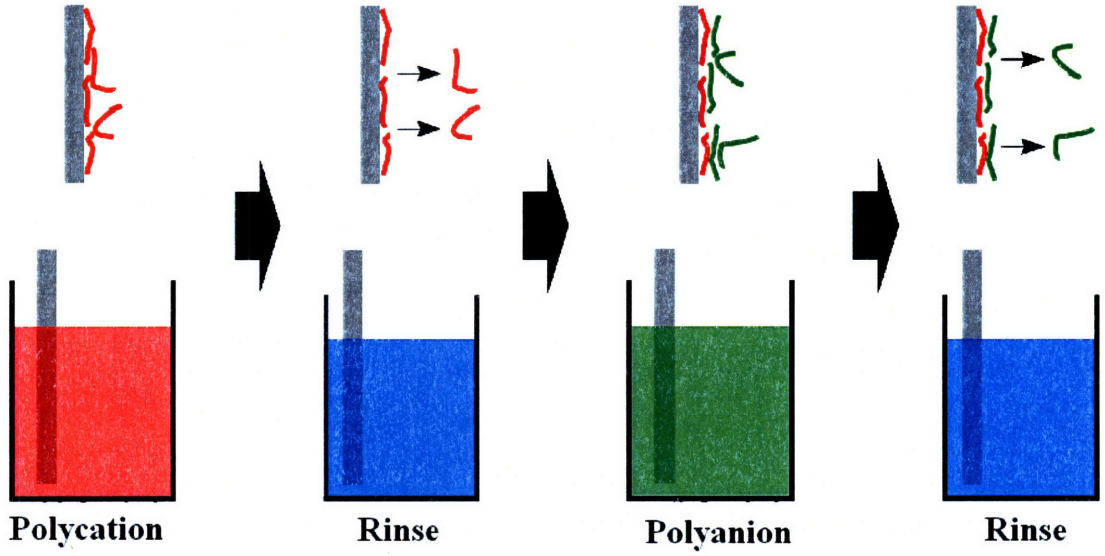


**Figure 1.** LbL growth process for a negatively charged substrate. If the substrate were to be positively charged, the polycation and polyanion in the figure would be switched.

The LbL method consists of dipping a charged substrate, such as a negatively charged soda-lime glass slide, into an oppositely charged polyelectrolyte or nanoparticle solution. The slide is then rinsed in water or other solutions to remove excess solute on the slide,

and the slide is left with a single layer of charged polymer or nanoparticles. This slide is then dipped in a solution containing an oppositely charged material and then rinsed again. This creates the first bilayer. This process can be repeated for as many bilayers as necessary.

The pH at which PEMs are assembled determines their stability. Using poly(acrylic acid) (PAA) and 3-aminopropyl modified silica nanoparticles($APSiO_2$) as a model, the difference in most common electrostatic charge at pH 3 and pH 7 is shown in Figure 2. This is due to the pKa value of the carboxylic acidic acid groups of PAA and the amine groups of $APSiO_2$. A pKa value is the pH at which a molecule or material has a fifty percent chance of being protonated. Below that pH, the molecule has a higher probability of being protonated, while above the pKa, the molecule has a lower chance of being protonated. As the pH is increased, the charge density on PAA increases, while the charge density on $APSiO_2$ decreases. Stable films can be grown between pH 2 and pH 4. However film stability is largely pH dependent. Furthermore, charge density dependence on pH is important in this experiment because counter-ions were added at pH 7 to interact with carboxylic acidic groups. Figure 3 shows a single bilayer of PAA/$APSiO_2$ on a negatively charged substrate. The positively charged $APSiO_2$ binds to both the negatively charged PAA and substrate.

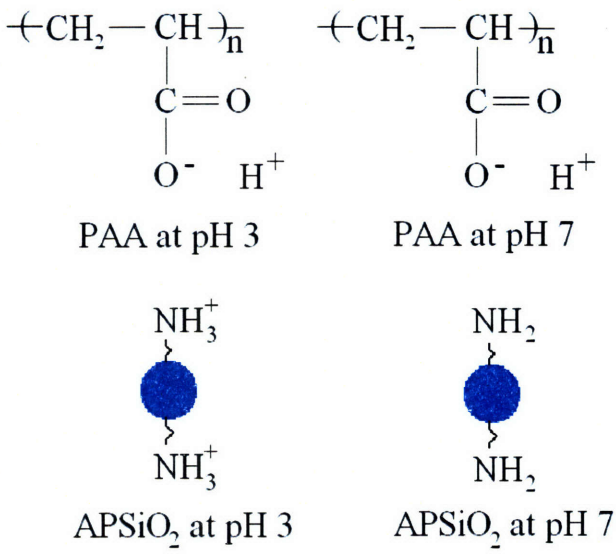


**Figure 2.** Polyectrolyte charge dependence on pH. Molecules shown are the most likely state of that molecule (either protonated, neutral, or deprotonated) at the pH indicated.

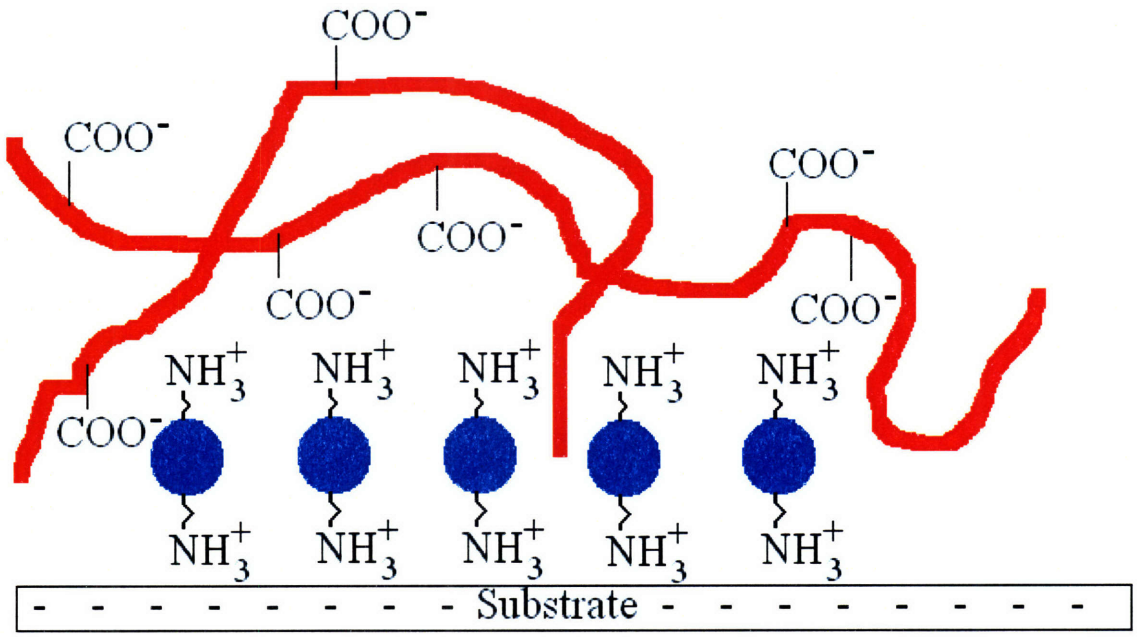


**Figure 3.** APSiO2/PAA film on negatively charged substrate (one bilayer).

PEMs have been grown and modified to create and increase antifogging properties of the films, and research groups have been able to produce various PEMs that have demonstrated robust anti-fogging.[1] Fog is produced when fluid condenses on a film in discrete droplets that can scatter light. When the contact angle, defined by the angle

satisfying Young's equation made by the fluid and the surface, is low, light scattering events do not occur and the film will transmit light. However, when the contact angles are high, droplets form and scatter light effectively, creating a foggy appearance.[2] A high energy surface that is roughened will be able to form a continuous or near-continuous film of liquid on the surface, diminishing the amount of fog created.[3]

This has been done by creating superhydrophilic surfaces that exhibit nanoporosity. The superhydrophilicity of the film creates the anti-fogging property by inhibiting the formation of water droplets that would scatter light. The nanoporosity of the film ensures that the water can wick into the multilayer system rather than simply spreading on the surface. It is this wicking that gives the film the superwetting characteristic, producing water contact angles of less than 5 degrees on the film. Films of poly(allylamine hydrochloride) (PAH) and $SiO_2$ nanoparticles have been investigated by Cebici et. al. that support the theory that nanoporosity in a hydrophilic PEM can greatly aid wetting properties. Findings suggest that superwetting occurs when water fills the surface microstructure.[1] The Rubner group has further investigated the PAH/ $SiO_2$ films, using the $SiO_2$ nanoparticles of different size to create the desired nanoporosity in films. Unpublished results find that the superwetting properties are created by capillary imbibition of water droplets into the nanoporous structure of the film. Instead of simply filling in the nanopores, however, the water builds up as shells around nanoparticles. Capillary condensation, the process by which fluid is moved and confined to nanopores due to the lower pressure created in those nanopores, is the cause of the wicking that inhibits water droplets from forming. Good anti-fogging properties have been observed with the PAH/ $SiO_2$ films.

However, these films do not retain their antifogging properties after aging in a humidity chamber. The Rubner group has also studied another type of film that does retain its antifogging properties even after humidity aging for 3 days. PAA/ $APSiO_2$ films grown on glass have been shown to have more durable antifogging properties. The difference between the PAH/ $SiO_2$ films and the PAA/ $APSiO_2$ films is that in the former, the polymer contains the positive charge, whereas the polymer contains the negative charge in the latter. This reversal on soda lime glass produces a denser packing for the PAA/ $APSiO_2$ films, which leads to lesser porosity but surprisingly greater antifogging longevity.

However, there is an ongoing search for a long-lasting durable film that will retain its antifogging properties after a long term humidity test on all commercially relevant substrates. While $APSiO_2$/PAA films perform well in a 3-day humidity aging test on glass, they are not yet as long-lived on polycarbonate and quartz.

## 1.2 Project Goals

### 1.2.1 Thesis Objectives

The objective of this thesis is to observe the effect of titrating carboxylic acidic acids in PEM structures with various counter-ions (e.g. $Na^+$, $Li^+$, $K^+$, $Mg^{2+}$, $Ca^{2+}$, and $Ba^{2+}$). Specifically, titrating PEM structures with highly hydrophilic counter-ions should impart or improve the anti-fogging effects or film wettability. Another objective of this thesis is to observe the effect of various counter-ions on the mechanical durability of the film.

### 1.2.2 Thesis Motivation

Antifogging coatings will have an enormous commercial and safety impact on today's world. Improved antifogging coatings would be used on windshields, eyeglasses, safety

glasses, windows, and ski and SCUBA goggles. Furthermore, antifogging coatings would help reduce inefficiencies in greenhouse windows and solar arrays.[2] Specifically, this thesis focuses on retaining antifogging properties after humidity aging. Antifogging films that have a long antifogging property lifetime in high humidity and high temperature conditions can be used for medical instruments and microscopes for *in vivo* operations.

### 1.2.3 Current Research Advancements

The current research attempts to understand what effect adding counter-ions as an additional modification step to the pre-existing PEM will have on hydrophilicity and wetting. This was done by modifying the pre-existing PEM structure with monovalent and divalent cations and observing the change in antifogging properties. If the addition of ions aids the superwetting and wicking characteristics of these films, it may greatly impact the design of future PEMs. The cations interact with the carboxylic acid groups from the PAA, as shown in Figure 4. The cations may provide some extra hydrophilic characteristics, and may improve antifogging properties after humidity aging. Furthermore, the divalent cations may provide a source of internal cross-linking and enhance the mechanical stability of these films.

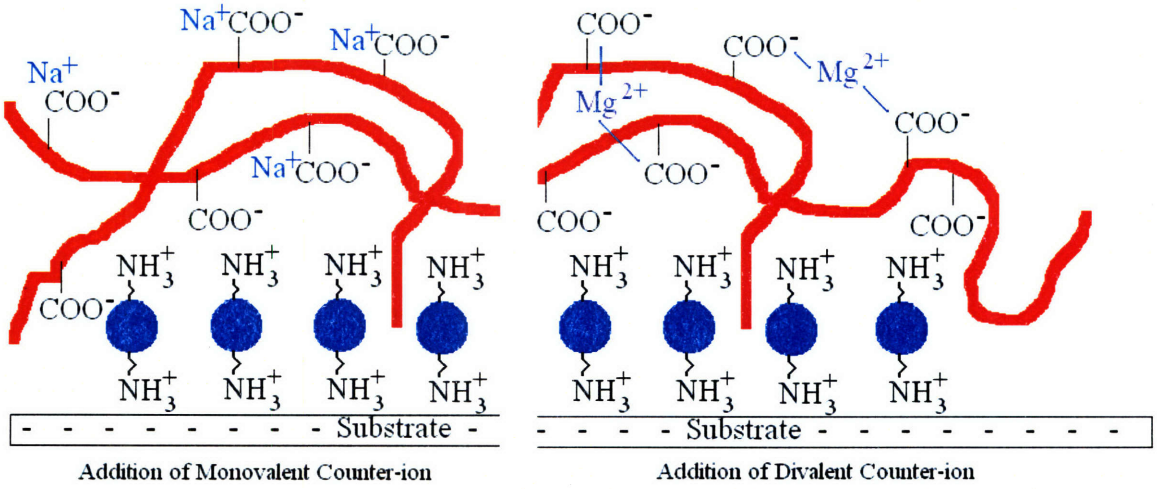


**Figure 4.** Introduction of cations to $APSiO_2$/PAA film

# Chapter 2: Design Parameters

## 2.1 Introduction to Design Idea

This project proposes to increase anti-fogging behavior in PEM films by the addition of cations. The PEM studied is a multilayer of $APSiO_2$ nanoparticles and PAA. Under various synthesis pHs of these films, the PAA films will contain different amounts of free carboxylic acid groups. When these PEMs are dipped in salt solutions, the free carboxylic acid groups will interact with the counter-ions. The adsorbed counter-ions will give the PEM a new antifogging characteristic depending on the new hydrophilicity of the film. In addition, divalent cations may interact with multiple carboxylic acid groups, promoting cross-linking and a higher mechanical stability and durability. However, prior to dipping PEMs in counter-ion solutions, it was important to find a stable PEM system to use for this experiment.

## 2.2 Exploratory Experimentation

### 2.2.1 Thickness Consideration and Calibration

The thickness of the grown films should be consistent in order to ensure proper comparisons across different systems. A thickness of 100 nm was chosen as a suitable thickness to preserve optical transmittance and interference color differentiation. At around 100 nm, the PEM film takes on a purple hue. However, the interference color behaves in a sinusoidal manner with relation to thickness, and it is easy to observe perturbations in thickness by the interference color observed in the film.

### 2.2.2 Free Carboxylic acidic acid Group Content

Counter-ions will adsorb to the film at sites in which there are free carboxylic acid groups available in the PAA layers. Experimentally, it is important for a large amount of free

carboxylic acidic acid groups to be present in the films so counter-ions may interact with them in order to clearly observe the effect the counter-ions have on antifogging properties. Although all carboxylic acidic acid groups may not interact with counter-ions, it was important to choose a PEM system that had the most free carboxylic acidic acid groups in order to attract the largest number of counter-ions.

In order to determine the free carboxylic acidic acid group content of the films, they were stained with methylene blue (Figure 5). Methylene blue is a blue dye which binds to negative charges, and based on the density of the dye, will help determine the relative amount of free carboxylic acid groups. As the films are dipped in methylene blue solution, the positively charged nitrogen in the methylene blue interacts with free carboxylic acid groups and the dye molecule is adsorbed to the film.

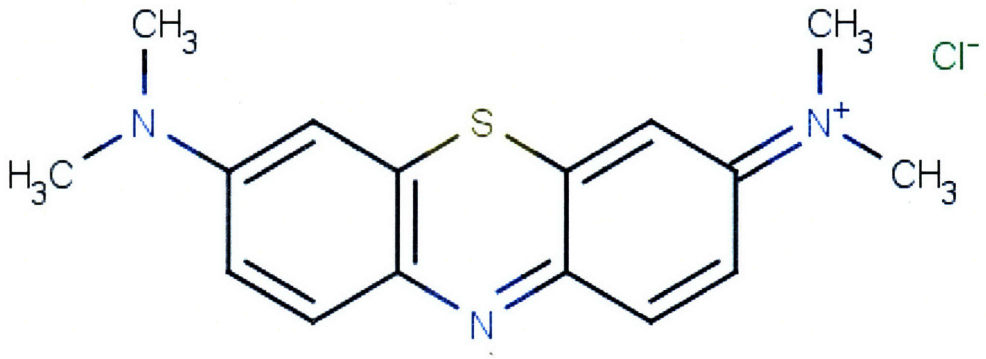


**Figure 5.** Methylene blue molecular structure.

2.2.3 Film Stability Under pH Stress

It was important to observe the stability of the PEM system under various pH stresses before carrying out the counter-ion experiments. Films that degrade under pH conditions other than that in which they were made are not as suitable for the counter-ion test, because it is important to introduce the counter-ions at a neutral pH in which they would bind to the free carboxylic acid groups more abundantly.

## 2.3 Exploratory Experimental Methods

### 2.3.1 PEM Films on Glass Slides

Initially, PEMs of $APSiO_2$/PAA were grown on clean glass slides (VWR microslides, premium, plain from VWR). The slides were cleaned by sonication in solutions of soap-water, 1M NaOH, and milliQ DI water for 15 minutes, 15 minutes, and 5 minutes respectively. In order to test different systems of PEMs, they were grown with different pH solutions of $APSiO_2$ and PAA. The systems tested were at pH 3.0, pH 2.5, and pH 2.0. Solutions of $APSiO_2$ were made by dissolving 4.0 g $APSiO_2$ in 500 mL milliQ DI water and titrating to the correct pH with HCl (Hydrochloric Acid solution, 1.0 N from Sigma). Solutions of PAA were made by dissolving 0.14 g PAA (MW ~90,000, 25% aqueous solution from Polysciences Inc.) in 500 mL miiliQ DI water and titrating to the correct pH with HCl. Using a StratoSequence VI (nanoStrata Inc.) spin dipper and the StratoSmart v6.2 (nanoStrata Inc.) software, a bilayer film was grown by first dipping slides in the $APSiO_2$ solution for 10 minutes, followed by dips in three water rinses of equal pH as the solutions for 2 minutes, 1 minute, and 1 minute. This was followed by dipping slides in the PAA solution for 10 minutes, followed by dips in three water rinses of equal pH as the solutions for 2 minutes, 1 minute, and 1minute. To create more bilayers, this process was repeated. To find the number of bilayers in each system to reach the appropriate thickness of 100 nm, calibration curves were constructed. Film thickness was measured using the P10 Profilometer (Tencor).

### 2.3.2 Film Stability Under pH Stress

Due to the growth of these films under different pHs, the stability of each film was tested at various pHs. To identify disparities between the systems, a film of each was immersed

in water at pH 9.0, pH 6.0, pH 4.0 and their growth pH (3.0, 2.5, or 2.0) and the resulting film was observed by visual inspection for alterations in slide coverage and by profilometer thickness measurements.

### 2.3.3 Free Carboxylic acid Group Content

Free carboxylic acid group content was measured by method of methylene blue staining. Methylene blue solutions were made by dissolving 0.015 g crystalline Methylene Blue (Alfa Aesar) in 40ml yellow pH 7 buffer (BDH). Films were stained by immersing the slides in this solution for 15 minutes, followed by immersion in three rinses of milliQ DI water for 2 minutes, 1 minute, and 1 minute. One untreated PEM film of each pH system was stained with methylene blue, as were all films that were pH treated. The stained films were then analyzed using a Cary 500i Spectrophotometer (Varian, Inc.) to measure the relative absorbance around the blue wavelength.

## 2.4 Exploratory Experimental Results

Calibration experiments showed optimal number of bilayers on glass slides to be eight bilayers for a pH 3.0 system, seven bilayers for a pH 2.5 system, and six bilayers for a pH 2.0 system. Films did not show a linear response to additional bilayers, as can be seen in Figure 6. Unpublished results from the Rubner Group have also found that film growth for PEMs follow an exponential growth curve. Because the target film thickness was 100nm, additional points were not added to the calibration graph once this goal was reached.

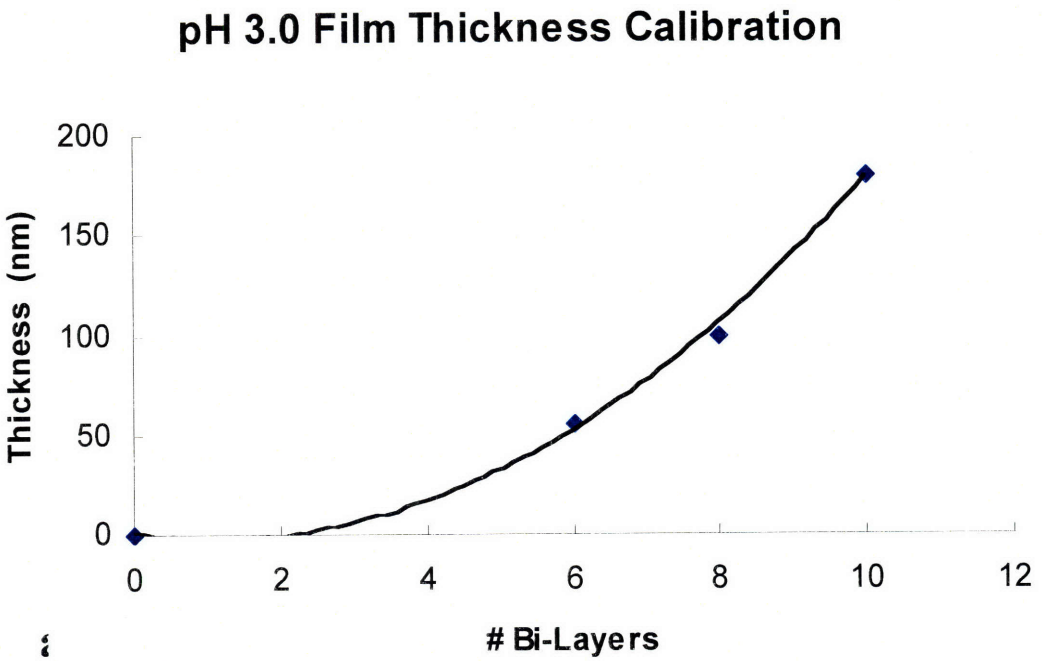
pH 3.0 Film Thickness Calibration
Thickness (nm)
200
150
100
50
0
0
2
4
6
8
10
12
# Bi-Layers

a

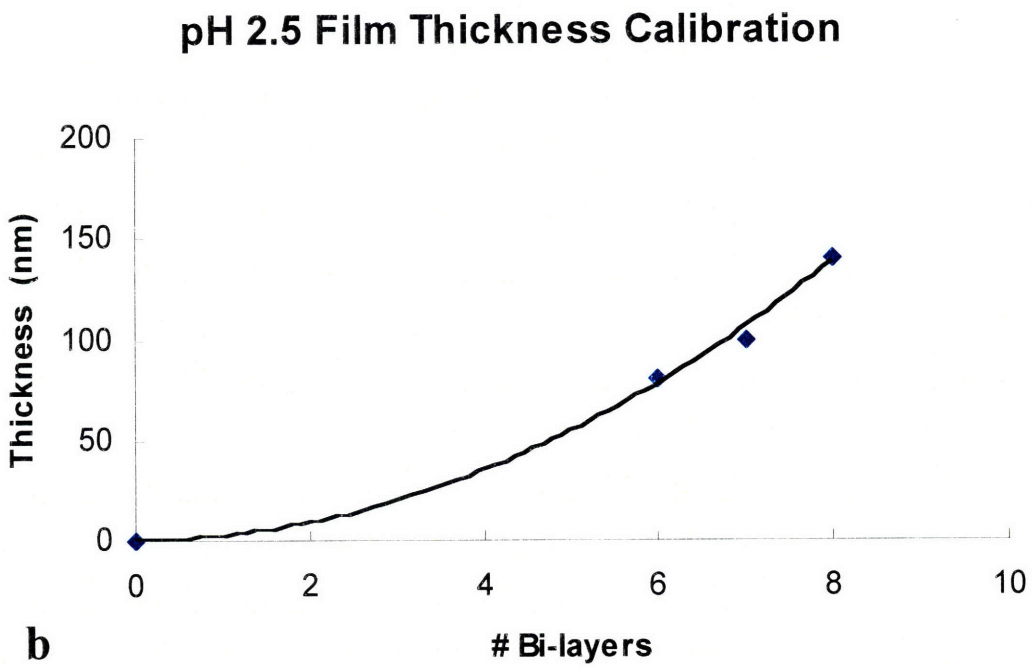
pH 2.5 Film Thickness Calibration
Thickness (nm)
200
150
100
50
0
0
2
4
6
8
10
# Bi-layers

b

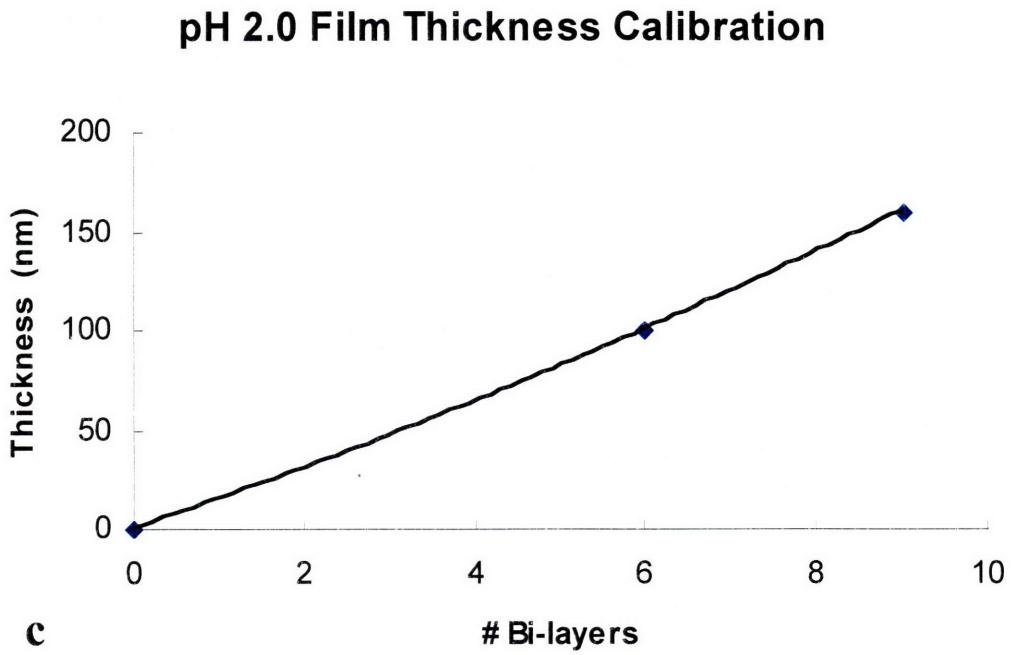


**Figure 6.** Calibration curves for films grown at a) pH 3.0, b) pH 2.5, and c) pH 2.0 with 2nd degree polynomial fitted trendline.

From the post assembly pH treatment studies on each of these systems, some de-lamination or degradation was observed for all films at pH 9.0. However, the films made at pH 3.0 showed very slight delamination around the slide, while the films made at the other two pHs showed marked film degradation. Table 1 lists the observations of the films upon removal from the pH dip. Figure 7 shows a series of pictures comparing different degrees of degradation in these films. These films were methylene blue stained in order to characterize their free carboxylic acid content, explaining the blue/purple tinge.

**Table 1.** Results of pH dips for different growth systems.

| Growth pH | Post assembly treatment pH | Result |
|---|---|---|
| 3.0 | 3.0 | No Change |
| 3.0 | 4.0 | No Change |
| 3.0 | 6.0 | No Change |
| 3.0 | 9.0 | Slight Delamination |
| 2.5 | 2.5 | No Change |
| 2.5 | 4.0 | No Change |

| | | |
|---|---|---|
| 2.5 | 6.0 | No Change |
| 2.5 | 9.0 | Considerable Degradation |
| 2.0 | 2.0 | No Change |
| 2.0 | 4.0 | No Change |
| 2.0 | 6.0 | Slight Degradation |
| 2.0 | 9.0 | Considerable Degradation |

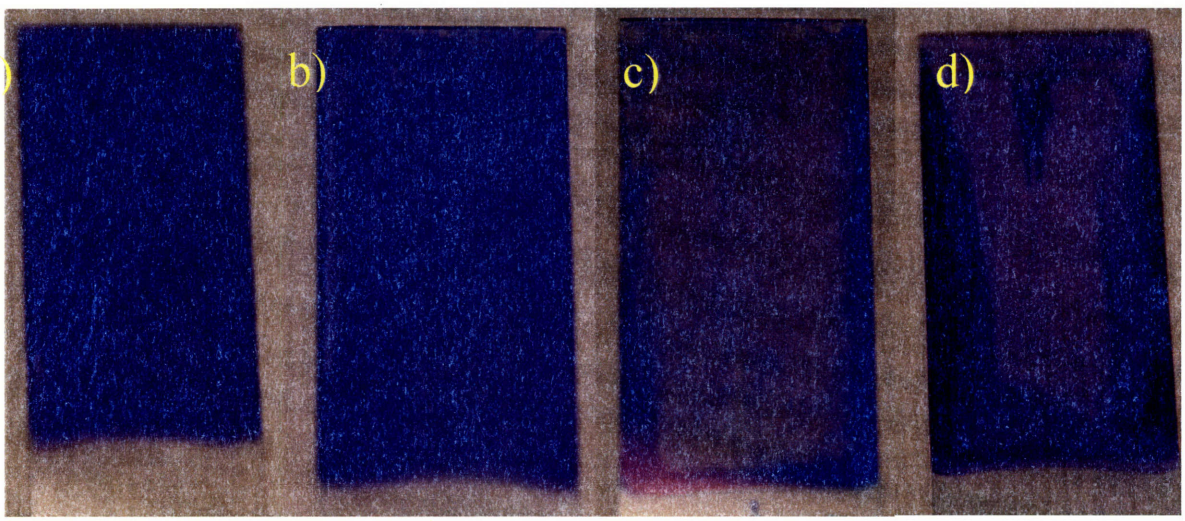


**Figure 7.** Degradation of pH treated films: a) growth in pH 3.0, treated with pH 6.0, b) growth in pH 3.0, treated with pH 9.0, c) growth in pH 2.5, treated with pH 9.0, and d) growth in pH 2.0, treated with pH 9.0.

Results of the methylene blue treatments and spectrophotometer measurements, shown in Table 2, show similar results for all films treated in growth (2.0-3.0) pH, pH 4.0, and pH 6.0. Each of these had an absorbance between 6.5 and 6.9 times the absorbance of an unstained film at 500 nm. While the difference between 6.5 and 6.9 times the absorbance may seem large, in fact small alterations in the placement of the film could result in absorbance changes of up to 0.6 times the absorbance of an unstained film.

**Table 2.** Methylene blue stained absorbance results of post-assembly treated films.

| Growth pH | Post assembly treatment pH | Relative Absorbance |
|---|---|---|
| 3.0 | none | 6.8 |
| 3.0 | 3.0 | 6.7 |
| 3.0 | 4.0 | 6.7 |
| 3.0 | 6.0 | 6.6 |
| 3.0 | 9.0 | 6.9 |
| 2.5 | none | 6.9 |
| 2.5 | 2.5 | 6.9 |

| | | |
|---|---|---|
| 2.5 | 4.0 | 6.8 |
| 2.5 | 6.0 | 6.7 |
| 2.5 | 9.0 | 6.3 |
| 2.0 | 2.0 | 6.6 |
| 2.0 | 3.0 | 6.7 |
| 2.0 | 4.0 | 6.7 |
| 2.0 | 6.0 | 6.5 |
| 2.0 | 9.0 | 5.8 |

### 2.5 Experimental Setup Conclusions

Free carboxylic acid group content was not significantly different for all systems after treatment in pH 6.0, and de-lamination and degradation occurred in all systems for dips in pH 9.0. However, the amount of degradation was least in films made at pH 3.0, and this system was determined to be the best to observe the counter-ion influence on antifogging PEMs.

## Chapter 3: Counter-ion Influence on Antifogging PEMs

### 3.1 Polyelectrolyte Films on Polycarbonate Slides

PEMs of APSiO2/PAA were grown on plasma cleaned polycarbonate slides. The slides were plasma cleaned by engulfing the slides in oxygen gas at 400 mTorr and creating an ionizing electric field for ten seconds. Films were grown using the same method as on glass slides, and a calibration curve was constructed to find the correct number of bilayers to get the appropriate 100nm thickness. Polycarbonate was chosen as a substrate because of the demand for its use in commercial applications. Applications that specifically would benefit from antifogging coatings include eyeglasses and sunglasses, car headlights, and various medical devices.

### 3.2 Counter-ion Substitution

0.1M solutions of NaCl (from Sodium Hydroxide, 1.000 – VWR), LiCl (from Lithium Hydroxide, Reagent grade, ≥98%, powder from Sigma Aldrich), and KCl (from Potassium Hydroxide, Pellets, 99.99% metals basis, semiconductor grade from Sigma Aldrich), and 0.05M solutions of $MgCl_2$ (from Magnesium Hydroxide, Ultra >99% from Fluka), $CaCl_2$ (Calcium Hydroxide puriss. from Riedel-deHaën), and $BaCl_2$ (Barium Hydroxide, tech., ~95% from Aldrich) were made and titrated to a pH of 7. The PEM films dipped on polycarbonate slides at pH 3.0 were immersed in these salt solutions for an hour, after which they were immersed in a milli-Q DI water rinse for 15 minutes. At the pH the dip was conducted at, and, later, at ambient conditions, it appeared that the magnesium particles precipitated and is the cause for the cloudy nature of the film. Even under room temperature and humidity, the $Mg^{2+}$ film was noticeably cloudy, so the effect of introducing magnesium counter-ions to a PEM film must be deemed inconclusive, and the results were removed from the results section. In order to prevent precipitate from forming, the salt solutions may be brought to a lower pH. This would decrease the amount of magnesium salt precipitate formed.

### 3.3 Film Characterization

#### 3.3.1 Anti-Fog Test

Anti-fog tests were performed on all the films to ascertain their anti-fogging characteristics. This test consisted of introducing the PEM film to high humidity and high temperature conditions (80% humidity and 37°C) and taking photographs after 0, 10, and 20 seconds using a Fujifilm camera.

### 3.3.2 Contact Angle Measurement

Contact angle measurements were taken with a VCA2000 Video Contact Angle System (AST Inc.) goniometer using the dynamic mode of the VCA OptimaXE (AST Inc.) software. The contact angles were measured by dropping a single droplet of water onto the PEM film and measuring the angle the droplet made with the surface. Contact angles were measured at the time the droplet hit the surface and at 0.1 second intervals up to half a second, as well as the contact angle after approximately three seconds.

### 3.3.3 Durability Test

A mechanical durability test was applied to the films by rubbing them with a KimtechScience Kimwipe (Kimberly-Clark Professional). They were each rubbed gently by hand and then more forcibly until an inference of relative stability could be made about the film.

### 3.3.4 Humidity Chamber Aging

After these tests were performed, the films were aged in the high humidity and high temperature chamber (80% humidity and 37°C) for three days. After each day, anti-fog tests and contact angle measurements were repeated.

### 3.3.5 Ellipsometry Measurements

Measurements were taken of each film with a XLS-100 (J.A. Woollam Co., Inc.) spectroscopic ellipsometer to ascertain the thickness and refractive index. The ellopsometer was powered by a M-2000D (J.A. Woollam Co., Inc.) power source, and ran with the Wvase32 (J.A. Woollam Co., Inc.) software package. The scans were taken at a 70 degree angle and from a wavelength of 250nm to 40000nm.

### 3.4 Results

Contact angle measurements were taken from pre-aged films until the third day of aging in the humidity chamber. Figure 8 shows the contact angles of a drop of water on the film from the moment a drop touched the film surface until half a second afterwards. The four graphs represent pre-aging through three days of humidity aging, and each contain data from the six counter-ions tested as well as an unaltered 10 bilayer $APSiO_2$/PAA film. Before the films are placed in the humidity chamber, day zero, all modified films show superior hydrophilicity to the unaltered film, as shown by their smaller contact angles. After one day in the humidity chamber, the films modified by monovalent cations show superior hydrophilicity to the unaltered film, while the divalent cations exhibit less hydrophilic character than the unaltered film. By day two in the humidity chamber, the trend seen in day one is seen more pronouncedly: the films modified by monovalent cations exhibit an inverse relation between size and hydrophilicity, and continue to show significantly higher hydrophilic character than the unaltered film. Also, after two days in the humidity chamber, the films modified by the smaller divalent cations, $Mg^{2+}$ and $Ca^{2+}$, have comparable or slightly lower contact angles than the unaltered film. After three days in the humidity chamber, the monovalent cation-modified films show comparable contact angle measurements to each other half a second after the water droplet makes contact with the film, and are still significantly more hydrophilic than the unaltered film. Similarly, the smaller divalent cations continue to have comparable contact angles to the unaltered film, while the $Ba^{2+}$ -modified film continues to exhibit a lesser degree of hydrophilicity.

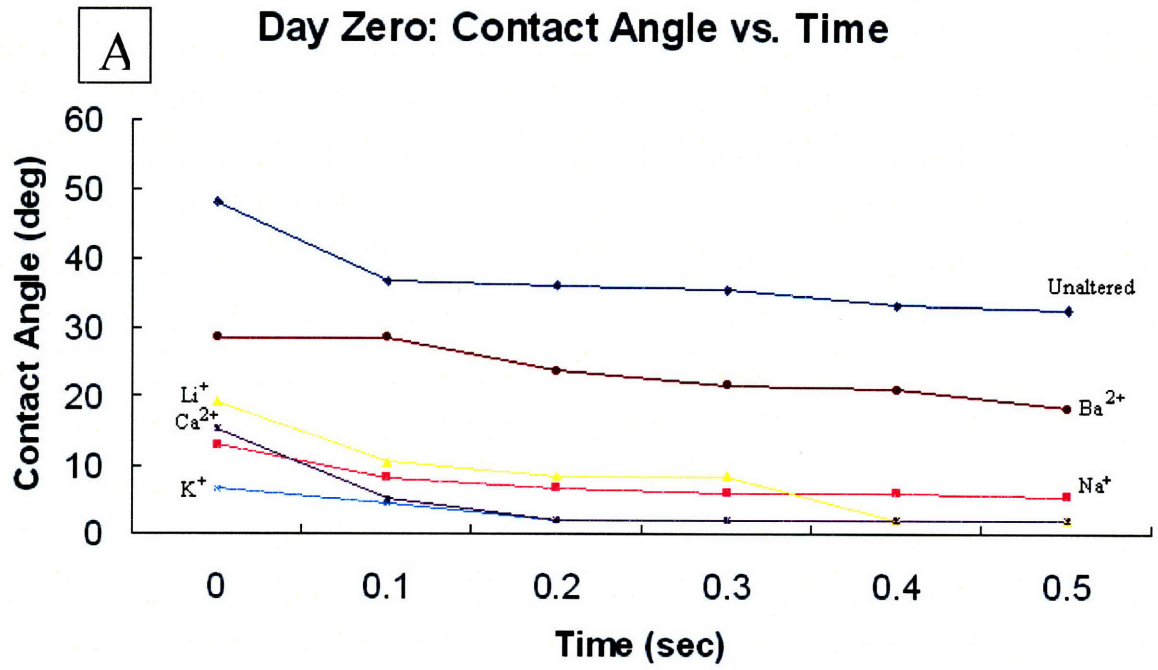
A
Day Zero: Contact Angle vs. Time
Contact Angle (deg)
60
50
40
30
20
10
0
0
0.1
0.2
0.3
0.4
0.5
Time (sec)
Unaltered
Ba2+
Li+
Ca2+
K+
Na+

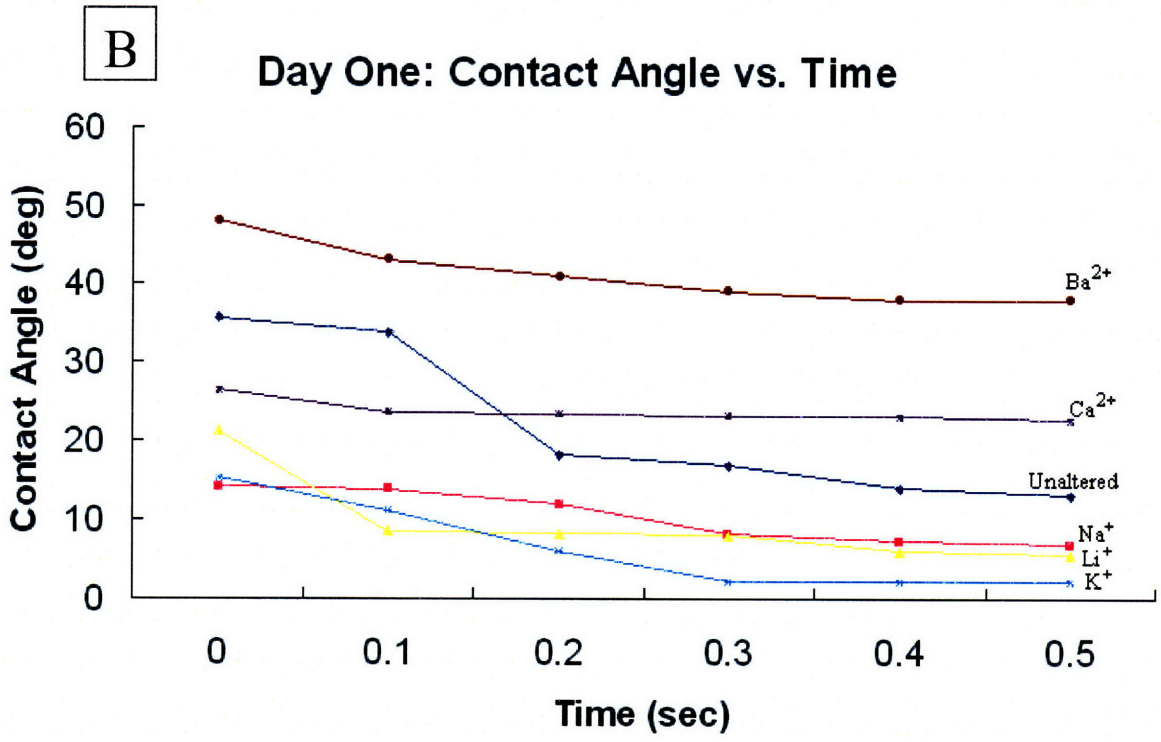
B
Day One: Contact Angle vs. Time
Contact Angle (deg)
60
50
40
30
20
10
0
0
0.1
0.2
0.3
0.4
0.5
Time (sec)
Ba2+
Ca2+
Unaltered
Na+
Li+
K+

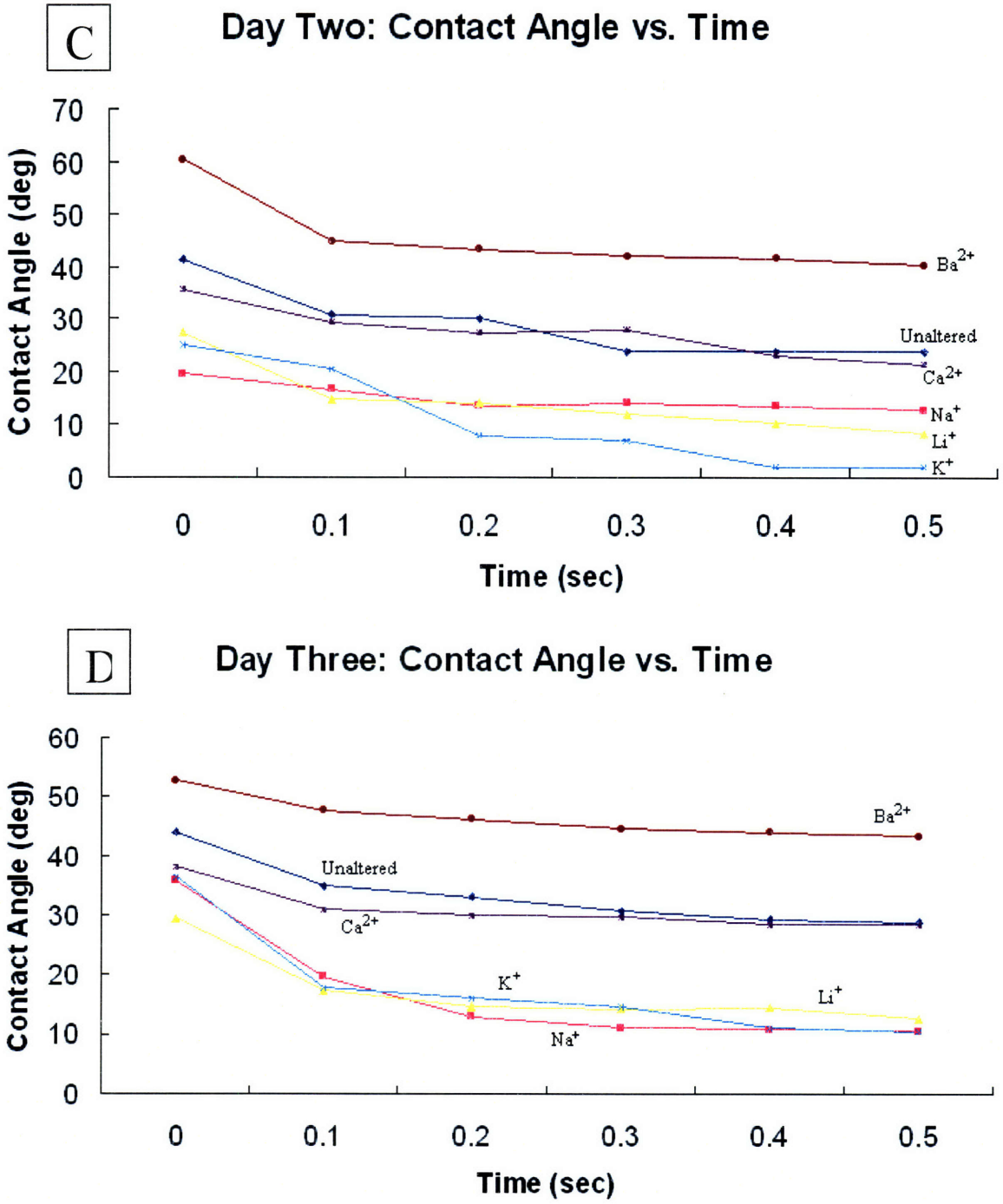


**Figure 8.** Dynamic contact angles of counter-ion dipped films from 0 – 0.5 seconds after water droplet contact after a) no aging, b) one day aging, c) two day aging, and d) three day aging in humidity chamber.

Figure 9 shows the contact angles on the seven films after the water droplet had been in contact with the film for approximately three seconds as a function of humidity aging time. The films modified by monovalent cations have significantly lower contact angles

than the unaltered films despite aging. As observed earlier, the larger monovalent ions seem to correlate with increased hydrophilicity and lower contact angle. Furthermore, the monovalent cation-modified films do not have a large change in contact angle under the humidity aging. On the other hand, films containing divalent cations showed noticeably increased contact angles after due to aging.

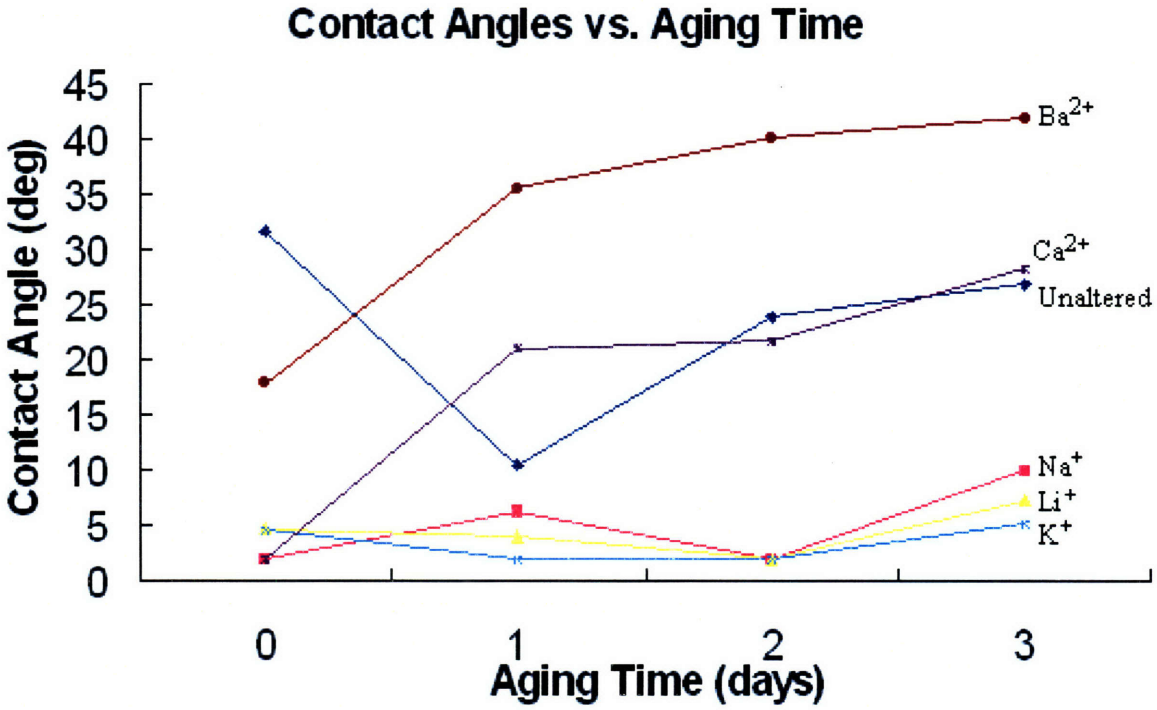


**Figure 9.** Final contact angles of counter-ion dipped films from zero to three days of aging in humidity chamber.

Table 3 shows the results of the anti-fog tests before, during, and after humidity aging for three days. The anti-fog tests show very good anti-fog properties for all films. However, after aging, the divalent cation-modified films lose their anti-fog property more quickly than the unaltered film. While the $Na^+$-modified film performed worse after 2 days of aging than the unaltered film, both the $Li^+$- and $K^+$-modified films performed better or on par after both one and two days of aging. Table 3 also shows evidence to counter the argument of antifogging dependency on contact angle (shows in parentheses in Figure 2). Typically it has been observed that with <5 degree water droplet contact angles, films

show superb antifogging characteristic.[1,2] However, the data here suggests that antifogging properties may be more dependent on some other feature of a film, as there is not strong correlation between antifogging properties and the contact angle. Figure 10 shows a comparison of the unaltered film, the $Na^+$-modified film, and the $Li^+$-modified film after two days of humidity aging. We see that $Li^+$-modified films may have outperformed the unaltered film in the anti-fog test over time.

**Table 3.** Development of anti-fogging properties over humidity aging time (contact angles in degrees in parentheses)

| Film | Antifogging | 1 Day | 2 Day | 3 Day |
|---|---|---|---|---|
| Unaltered | very good (32) | good (10) | middle (24) | middle (27) |
| Na | very good (<5) | good (6) | bad (<5) | bad (10) |
| Li | very good (<5) | very good (<5) | good (<5) | middle (7) |
| K | very good (<5) | very good (<5) | middle (<5) | bad (5) |
| Ca | very good (<5) | bad (21) | bad (22) | bad (28) |
| Ba | very good (18) | good (36) | bad (40) | bad (42) |

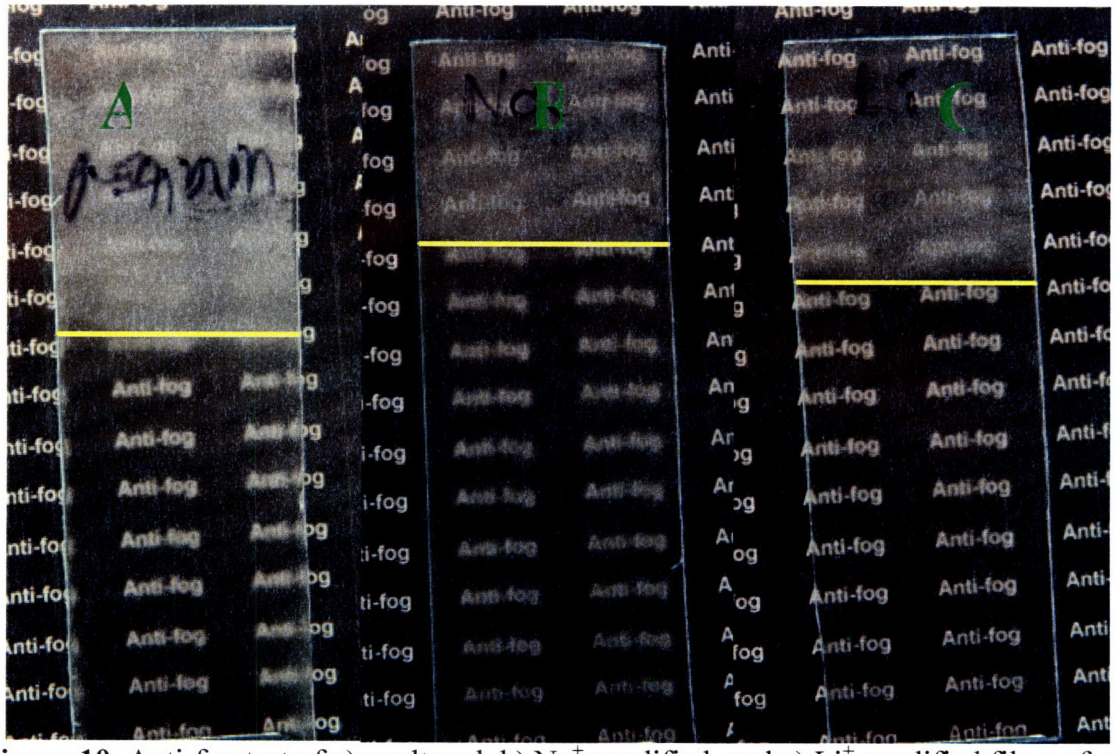


**Figure 10.** Anti-fog test of a) unaltered, b) $Na^+$-modified, and c) $Li^+$-modified films after two days of aging in the humidity chamber.

The mechanical durability was tested with a Kimwipe rub test. Table 4 shows the durability on a scale of 1 to 10, with a rating of 1 meaning the film was virtually impossible to rub off with the load of a human finger enclosed by a Kimwipe fully pressed against the film, and a rating of 10 meaning the film easily flaked off. Because all of the films were very durable, a rating of 2 or 3 meant that the film rubbed off under medium load from the finger. Most of these films did not damage or damage greatly under the rub test, and all of them showed good strength. There also seems to be no trend associated to durability that can be attributed to any specific aspect of these cations.

**Table 4.** Mechanical durability of counter-ion films under rubbing test

| Film | Observation | Numerical Rating |
|---|---|---|
| **Unaltered** | Extremely Durable | 1 |
| **Na** | Very Durable | 2 |
| **Li** | Extremely Durable | 1 |
| **K** | Very Durable | 2 |
| **Ca** | Durable | 3 |
| **Ba** | Extremely Durable | 1 |

Table 5 shows the thicknesses and refractive indices of the films from ellipsometry data before and after humidity aging. Although no significant trends can be observed in the pre-aged and post-aged thicknesses, there is a trend to be noticed in the refractive indices of the films. It appears that the films with monovalent cations have lower refractive indices, while the divalent cation containing films have higher refractive indices. We can hypothesize that the films with lower refractive index have increased porosity, and the air ($n = 1.00$) permeating these pores is bringing the overall refractive index of the film down. Similarly, comparing the divalent modified films with the unaltered films leads us to suggest that the higher refractive index of the divalent modified films shows lower

porosity and may indicate cross-linking may have occurred, encouraging a denser film with lower porosity. Table 6 shows the same ellipsometry data, but without a modeled roughness layer. This roughness layer is put in to account for film porosity that affects the refractive index. The roughness layer is modeled to be half air, half film material. The similarity between the two shows that there is likely at least a semi-uniform structure throughout the layers of the film. If this were not the case, the refractive indices would be largely different between the two tables.

**Table 5.** Film thickness and refractive index pre- and post-humidity aging with an included modeled semi-porous roughness layer

| | Unaged Roughness Layer Thickness | Unaged Film Total Thickness | Aged Roughness Layer Thickness | Aged Film Total Thickness | Unaged Refractive Index | Aged Refractive Index |
|---|---|---|---|---|---|---|
| **Unaltered** | 2 nm | 114 nm | 5 nm | 120 nm | 1.43 | 1.47 |
| **Na** | 0 nm | 115 nm | 10 nm | 112 nm | 1.35 | 1.41 |
| **Li** | 0 nm | 129 nm | 11 nm | 115 nm | 1.34 | 1.42 |
| **K** | 23 nm | 122 nm | 40 nm | 127 nm | 1.35 | 1.39 |
| **Ca** | 6 nm | 114 nm | 0 nm | 115 nm | 1.47 | 1.48 |
| **Ba** | 8 nm | 117 nm | 2 nm | 129 nm | 1.50 | 1.49 |

**Table 6.** Film thickness and refractive index pre- and post-humidity aging without modeled semi-porous roughness layer

| | Un-aged Thickness | 3 Day Aged Thickness | Un-aged Refractive Index | 3 Day Aged Refractive Index |
|---|---|---|---|---|
| **Unaltered** | 114 nm | 120 nm | 1.43 | 1.46 |
| **Na** | 116 nm | 114 nm | 1.35 | 1.40 |
| **Li** | 130 nm | 116 nm | 1.34 | 1.41 |
| **K** | 130 nm | 116 nm | 1.34 | 1.41 |
| **Ca** | 113 nm | 118 nm | 1.47 | 1.48 |
| **Ba** | 112 nm | 129 nm | 1.49 | 1.49 |

### 3.5 Discussion

Antifogging properties largely seem to correlate with low contact angle measurements. This supports the findings of Cebeci and coworkers and corroborates the idea of nanopores wicking moisture into the film to create robust antifogging properties.[1]

An interesting feature in this experiment is the difference between the effects of monovalent and divalent cations on the PEM film characteristics. Monovalent cations caused lower refractive indices which we attribute to supposed increased porosity. The foundation of the creation of this porosity is unclear, and literature supports two ideas. The first possibility is that the salt solution causes a rearrangement of the film.[4] When the salt solution is added, the ions may cause the PAA to coil around the nanoparticle, and allow the salts into the film. This rearrangement process may cause an increase in nanoporosity. Another theory is that the salt solution shields the charged electrolytes and cause a mass loss as PAA is removed from the film into solution.[5,6] In this scenario, nanoporosity would similarly be increased altering the packing density of the remaining film altering the refractive indices. From current data, it would be hard to choose between these two possibilities, and it is likely that both mechanisms are taking place in these films upon salt treatment. The divalent cations, on the other hand, caused higher refractive indices than in the untreated film which could be directly attributable to a lower porosity due to the higher density caused by ionic crosslinking. However, an explanation of why neither mass loss nor film rearrangement play a large role cannot be given with the current data. An AFM measurement of porosity would be very useful in clearing this up.

Antifogging properties are tied into the porosity of the film, as the porosity has a large factor in capillary condensation. The benefits from increased porosity can be seen in some of the antifogging tests conducted on the monovalent cation modified films, as they generally performed as well or better than the unaltered films.

Contact angles can, for the most part, be explained by changes in porosity as well. As the pores filled more quickly due to capillary condensation in the less porous films, their contact angles increased rapidly. Conversely, the more porous films took more time for their antifogging properties to degrade and their contact angles to increase. However, as aging time increases, all films inevitably lose their antifogging properties.

An outlier to the contact angle trend with porosity is the set of pre-aging contact angle data. Before aging, the treated films, including the divalent films, all had lower contact angles than the untreated film. In this case, is likely that the increased hydrophilicity of the film due to cation addition was still able to direct water molecules into the pores of the films. After aging, the nanopores may have become saturated, explaining the large change in contact angles of the divalent films.

# Chapter 4: Summary and Future Work

## 4.1 Thesis Summary

The effects of counter-ions on antifogging properties of PEMs was investigated in this thesis. Interesting differences were found between monovalent and divalent cationic effects on the films. Monovalent cations may prove to be useful in increasing antifogging durability. More importantly, from this study, it is clear that salt solutions have a definite impact on PEM films and their water droplet contact angles and antifogging properties and warrant further investigation.

## 4.2 Future Directions

The outcome of this work has posed some interesting questions about why these counter-ions act the way they do. A study to determine the nano-porosity and topography of

counter-ion treated PEM films using an atomic force microscope (AFM) may shed light on the film characteristic differences observed between the monovalent and divalent counter-ions. Furthermore, it may show why although the contact angles for the monovalent counter-ion treated films was consistently low with humidity aging, and indeed much lower than the untreated film, the anti-fogging properties were not as effected.

More work should also be done in pH control when adding these counter-ions. Particularly, magnesium has a low solubility in water, and may be more likely to dissolve and consequently interact with PEMs at lower pHs. The pH at which all of these counter-ions are added may make a significant impact in the adsorption ratio, and therefore a significant impact on the hydrophilicity and anti-fogging properties.

Another method of treating PEMs that could be tried with counter-ions is that of calcination. Heat treating these counter-ions may impact them in a beneficial way.

There are a variety of experiments that can arise from the findings of this thesis, and hopefully some of these will be undertaken in the search for durable anti-fogging films.

### 4.3 Bibliography

(1) F. C. Cebeci, Z. Wu, L. Zhai, R. E. Cohen, M. F. Rubner, *Langmuir* **2006**, *22*, 2856

(2) J. A. Howarter, J. P. Youngblood, DOI: 10.1002/marc.200700733

(3) R. N. Wenzel, *Ind. Eng. Chem.* **1936**. *28*, 988.

(4) A. Fery, B. Scholer. T. Cassagneau, F. Caruso, *Langmuir* **2001**, *17*, 3779

(5) S. T. Dubas, J. B. Schlenoff, *Macromolecules* **2001**, *34*, 3736

(6) D. Kovacevic, S. van der Burgh, A. de Keizer, M. A. Cohen Stuart, *Langmuir* **2002**, *18*, 5607

**APPENDIX A**

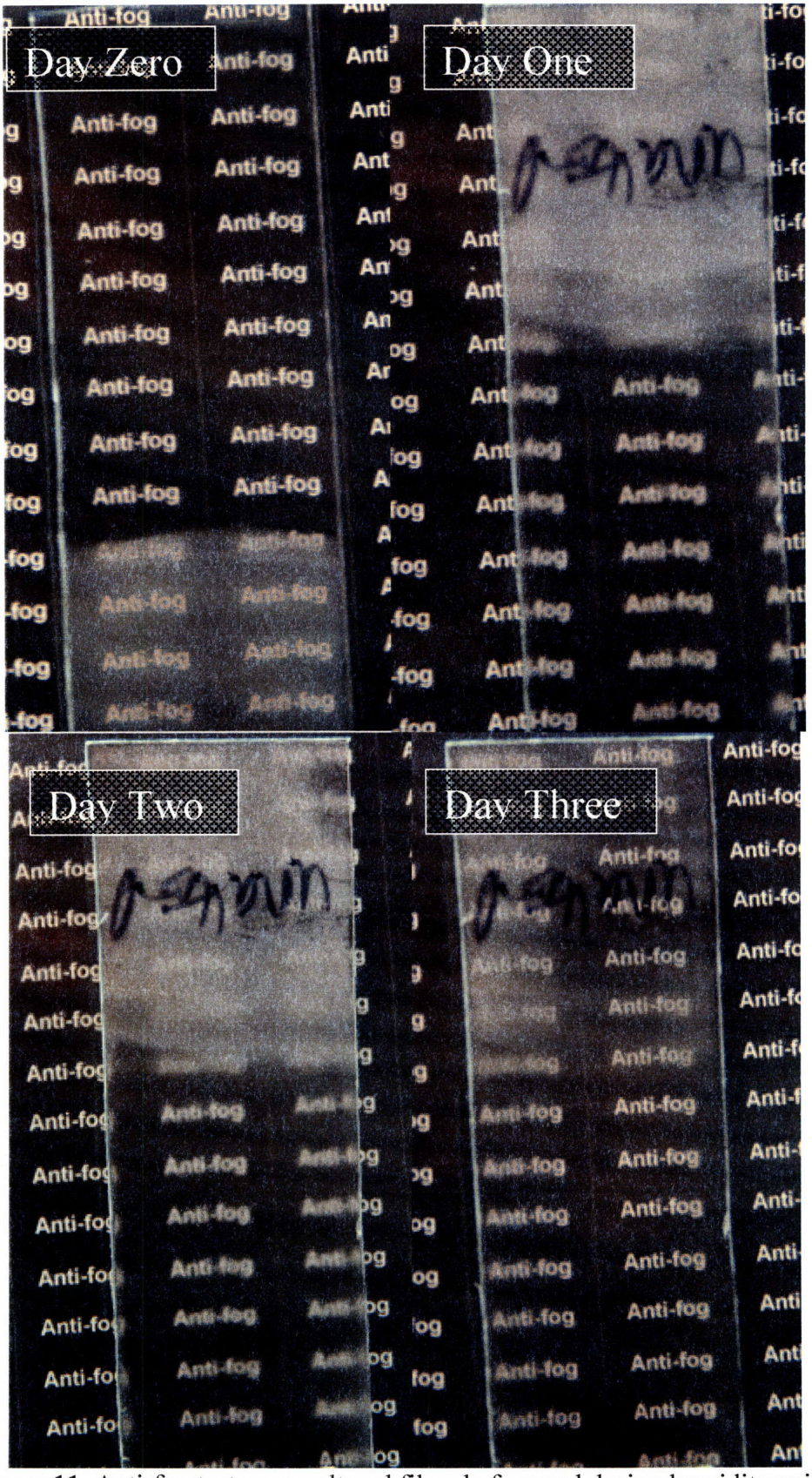


**Figure 11.** Anti-fog tests on unaltered films before and during humidity aging.


**Figure 12.** Anti-fog tests on Na-modified films before and during humidity aging.


**Figure 13.** Anti-fog tests on Li-modified films before and during humidity aging.


**Figure 14.** Anti-fog tests on K-modified films before and during humidity aging.

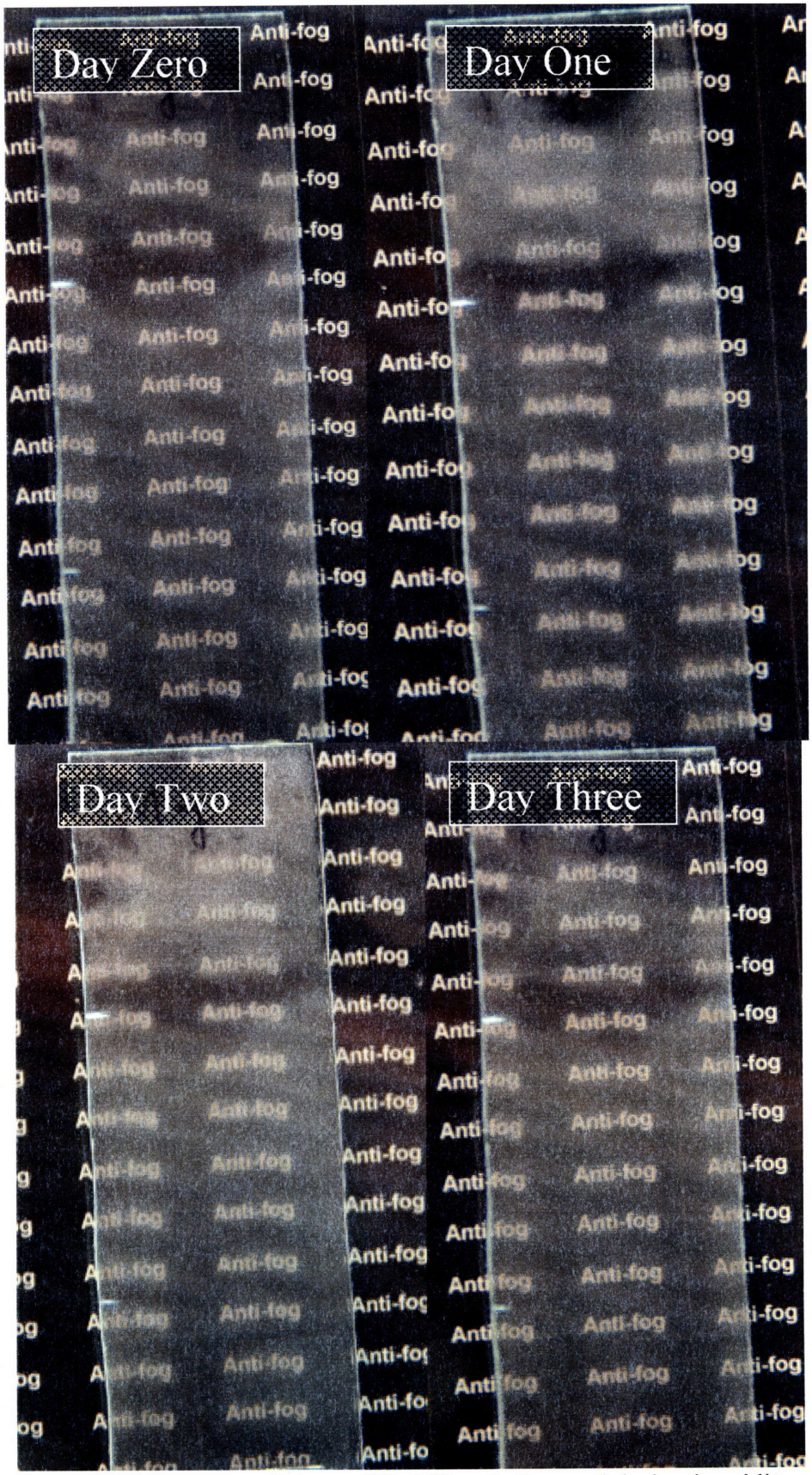


**Figure 15.** Anti-fog tests on Mg-modified films before and during humidity aging.


**Figure 16.** Anti-fog tests on Ca-modified films before and during humidity aging.


**Figure 17.** Anti-fog tests on Ba-modified films before and during humidity aging.